Annals of Nuclear Medicine Vol. 7, No. 2, 71–77, 1993

Optimization of Butterworth filter for brain SPECT imaging

Satoshi MINOSHIMA,*,*** Hirotaka MARUNO,* Nobuharu YUI,** Takashi TOGAWA,**
Fujimi KINOSHITA,** Masahiro KUBOTA,**** Kevin L. BERGER,***
Yoshitaka UCHIDA,* Kimiichi UNO* and Noboru ARIMIZU*

*Chiba University School of Medicine, Department of Radiology
**Chiba Cancer Center Hospital, Division of Nuclear Medicine
***University of Michigan, Division of Nuclear Medicine
****Toshiba Medical Corporation

A method has been described to optimize the cutoff frequency of the Butterworth filter for brain SPECT imaging. Since a computer simulation study has demonstrated that separation between an object signal and the random noise in projection images in a spatial-frequency domain is influenced by the total number of counts, the cutoff frequency of the Butterworth filter should be optimized for individual subjects according to total counts in a study. To reveal the relationship between the optimal cutoff frequencies and total counts in brain SPECT study, we used a normal volunteer and ^{99m}Tc hexamethyl-propyleneamine oxime (HMPAO) to obtain projection sets with different total counts. High quality images were created from a projection set with an acquisition time of 300-seconds per projection. The filter was optimized by calculating mean square errors from high quality images visually inspecting filtered reconstructed images. Dependence between total counts and optimal cutoff frequencies was clearly demonstrated in a nomogram. Using this nomogram, the optimal cutoff frequency for each study can be estimated from total counts, maximizing visual image quality. The results suggest that the cutoff frequency of Butterworth filter should be determined by referring to total counts in each study.

Key words: single photon emission computed tomography, Butterworth filter, brain, optimization, computer simulation

INTRODUCTION

RECENTLY, the performance of single photon emission computed tomography (SPECT) has been improved by development of ring-type or multiple-head camera systems.[1–4] High quality images can be obtained easily in a practical environment. However, without suitable image processing techniques, final reconstructed images cannot gain effective information from such high performance systems. Each step of image processing should be optimized to obtain maximum and constant image quality.

In SPECT imaging, images are degraded by the limited spatial resolution of the system and the superimposed random noise. In this study, we evaluate the Butterworth filter[5] as a pre-processing filter to reduce the random noise. The Butterworth filter is one of the "low-pass" filters which effectively reduce high frequency random noise in projection images. Two parameters determine the shape of this filter-order and cutoff frequency. Several reasons necessitate optimization of the Butterworth filter. Because of a different distribution volume in each subject, accumulation of tracer injected into a target organ differs from subject to subject even if the same dose is administered. With a fixed acquisition time per projection, this will cause different total acquisition

Received July 13, 1992, revision accepted October 7, 1992.

For reprints contact: Nobuharu Yui, M.D., Chiba Cancer Center Hospital, Division of Nuclear Medicine, 666–2 Nitona-cho, Chuoh-ku, Chiba 260, JAPAN.

counts in each study. Also, total counts will change according to acquisition time in different protocols. Injected radioactivity cannot be exactly the same for each subject. As the total counts determine the noise level in acquired images, the Butterworth filter must be optimized for each subject when maximizing effective information and reducing the random noise.

In clinical settings, parameters of the filter are usually decided by "trial and error", visually evaluating the quality of filtered images. Alternatively, optimal parameters can be estimated from individual acquired images because the random noise in nuclear images relates to total counts. A goal of this study is to clarify the relationship between total counts and optimal cutoff frequencies of the Butterworth filter using true brain SPECT data and computer simulation data and to discuss a practical approach to determine the optimal cutoff frequency.

THEORETICAL METHODS

A projection image can be expressed in the spatial-frequency domain under the assumptions of linearity and shift invariance as follows[6]:

$$G(u, v)=MTF(u, v)\cdot F(u, v)+N(u, v), \quad (1)$$

where G is an observed image, MTF is a modulation transfer function of the system, F is an original object, N is the superimposed noise, and u and v are spatial frequencies. MTF is a unique function under a certain imaging condition such as using the same camera, the same collimator, the same radionuclide, and a fixed object-collimator distance. Frequency distribution of the object is restricted to mainly low to medium frequency by this term. N is high frequency random noise inherent in the radioactive decay process, which power spectrum is equal to the total image count. The relationship between total counts and noise power spectra is demonstrated by a computer simulation in this study. Whole brain transaxial slice specimens of 1.5 mm thickness were digitized into a $256\times256\times76$ matrix. Assuming administration of 3 mCi (111 MBq) of N-isopropyl-p-[^{123}I]iodoamphetamine, gray/white matter ratio 4: 1, uniform attenuation coefficient 0.15 cm^2/gm, shift invariant system resolution full-width-at-half-maximum (FWHM) of 6.5 mm, detection efficiency of 2.5×10^{-4} photons transmitted/emitted, 30 second acquisition, projection image 64×64 matrix (left lateral view), and brain uptake of 4% to 16% (4% step) of the administered dose, lateral projection images with four different total counts were generated. Then, using a random-number generator, count-dependent Poisson noise was added to each projection image. The two-dimensional normalized power spectrum was averaged over annuli in frequency space and was displayed in Fig. 1. As the image counts (% uptake) increase, high frequency components due to the random noise decrease, and the object frequencies can be separated from the noise at the higher spatial frequency.

To reduce the high frequency noise component in projection images, the Butterworth filter is applied as a pre-processing filter prior to image reconstruction. The Butterworth filter is expressed as follows:

$$B(u, v)=1/(1+[(u^2+v^2)^{1/2}/Do]^{2n}), \quad (2)$$

where Do is the cutoff frequency, and n is the order of the filter which determines the steepness of the rolloff. At the cutoff frequency, the gain is down to 0.707, and higher frequency components are suppressed. As we have demonstrated that separation of the noise and the object frequencies is dependent on total counts of the acquired projection image, it is reasonable to determine the optimal cutoff frequency of the Butterworth filter according to the total counts in a study.

Criteria in optimizing the cutoff frequency vary with the aim of image interpretation. This means that quantitative and qualitative image interpretations will require different criteria for the optimization of filter function. In this study, the purpose of the optimization is to obtain the "best" image quality for visual image interpretation. For this reason, we used two indices: mean square error (MSE) calculated with a high quality image and visual evaluation of image quality by observers. These indices were assessed in final reconstructed images. A high quality image was created by projections with long acquisition time to reduce the random noise. The MSE is expressed as:

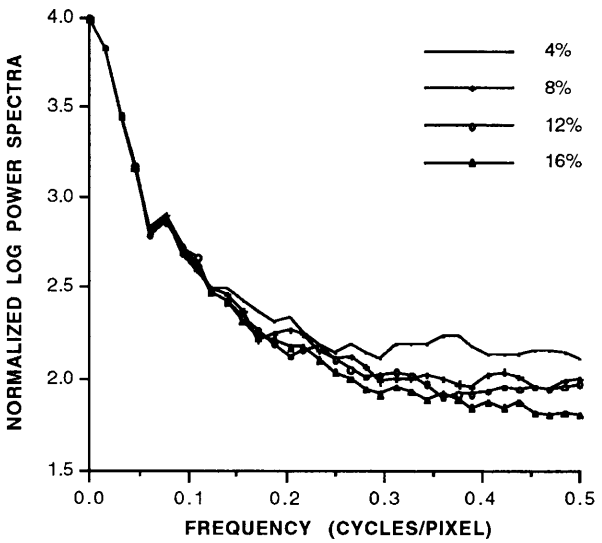

Fig. 1 Relationship between brain uptakes and power spectra in simulated lateral projections of the brain.

$$MSE = \sum\sum (g_{xy} - h_{xy})^2, \quad (3)$$

where g is the final image, h is the corresponding high quality image, and x and y are the pixel coordinates in the reconstructed images. The MSE represents how similar g is to h. The optimal cutoff frequency is determined by minimizing the MSE. Another index, visual evaluation of image quality, is completely subjective. Experienced observers judge reconstructed images processed by different cutoff frequencies and determine the most suitable cutoff frequency for visual interpretation.

If total counts and optimal cutoff frequencies have a constant relationship, optimal cutoff frequencies for individual cases can be reasonably estimated from a standard count-cutoff frequency nomogram. In this study, the relationship between the total counts and the optimal cutoff frequencies was examined by using the following materials and methods.

MATERIALS AND METHODS

Data acquisition and tomographic image reconstruction

After intravenous administration of 20 mCi (740 MBq) of ^{99m}Tc hexamethyl-propyleneamine oxime (HMPAO) to a normal volunteer, multiple sets of projections were obtained by the following method.

The subject's head was oriented in the scanner by laser guidance and fixed. The orbitomeatal (OM) line was approximately parallel to the scanning plane. Each projection set was obtained by a four degree step and one-hundred and twenty degree rotation (total 30 projections per camera, 90 projections per set) using a triple-head SPECT system (GCA-9300, Toshiba) with low-energy fan-beam collimators. The acquisition of fourteen sequential projection sets was started five minutes after the injection. Acquisition times for the projections were 10 seconds for the first twelve sets, 60 seconds for the 13th set, and 120 seconds for the 14th set. Thus, a total acquisition time of 300 seconds was achieved for each projection.

To minimize the effects of temporal changes in cerebral HMPAO accumulation during the data acquisition, acquired projection sets were summed to create five projection sets with different acquisition times by the following manner. A projection set with a 20-second acquisition was created by adding the 6th and 7th acquired projection sets. A projection set with a 40-second acquisition was created by adding the 5th, 6th, 7th, and 8th projection sets. A projection set with a 60-second acquisition was created by adding the 4th, 5th, 6th, 7th, 8th, and 9th projection sets. Projection sets with 80-second and 100-second acquisitions were created in the same manner. Five projection sets with acquisition times of 20, 40, 60, 80, and 100 seconds per projection were generated and used in the following analysis.

When reconstructing images, a projection set was transformed from four degree step acquisition, 256 × 256 matrix size to six degree step acquisition, 128 × 128 matrix size (pixel size 1.7 mm) by a fan-beam parallel transformation. Pixel counts were multiplied by sixteen prior to reconstruction. After applying a Butterworth filter, transaxial slices of 3.4 mm thickness were reconstructed using a ramp filter.[7] The order n of the Butterworth filter was fixed at 8 in this study.

High quality standard image

To create the high quality standard image for calculation of the MSE, all acquired projection sets were summed (total 300 seconds per projection). Twelve reconstructed images were generated using different cutoff frequencies of the Butterworth filter, 0.07 to 0.18 (0.01 step) cycles/pixel. A slice passing through the caudate head and the thalamus was chosen for analysis in this study. Two experienced observers evaluated the twelve reconstructed images in terms of the most suitable image quality for diagnostic image interpretation and decided on the high quality standard image.

Optimal cutoff frequency determined by MSE

Optimal cutoff frequencies for the five projection sets with different acquisition times were assessed by calculating the MSE from the high quality standard image. Butterworth filters of the cutoff frequencies from 0.07 to 0.18 (0.01 step) cycles/pixel were applied to each projection set, and slices corresponding to the high quality standard image were reconstructed. Normalized MSEs were calculated between each reconstructed image and the high quality standard image. The optimal cutoff frequency giving the smallest MSE was determined for each projection set.

Optimal cutoff frequency determined by visual inspection

Optimal cutoff frequencies for the five projection sets with different acquisition times were assessed by visual inspection. Instead of calculating MSEs, two experienced observers visually evaluated the reconstructed slices used in the previous section. An optimal cutoff frequency giving the most suitable image quality for diagnostic interpretation was determined for each projection set.

To make visual inspection more objective, we also evaluated four check points in all images: the cortical accumulation, the caudate visualization, the thalamic visualization, and the lingual gyri separation (Fig. 2).

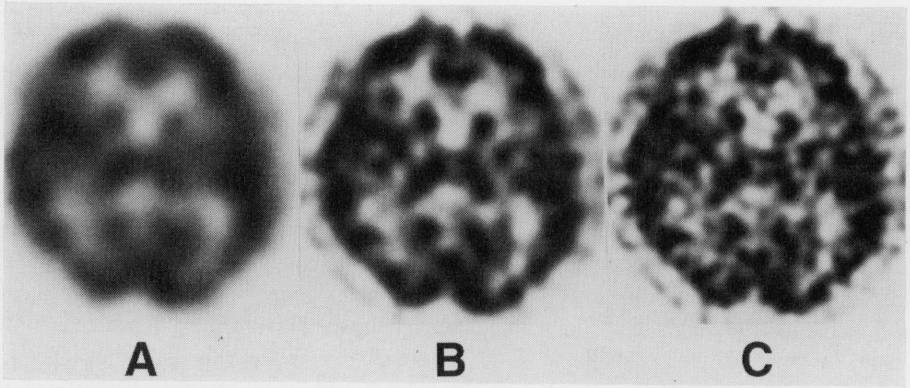

Fig. 2 Examples of visual inspection criteria. Images were created from a 100-second projection set with different filter functions. The cortical accumulation, the caudate visualization, the thalamus visualization, and the lingual gyral separation are classified into 1 (good) and 0 (poor). All of the four indices were evaluated as 0 in the images A and C, and 1 in the image B.

Suitable smoothing of the cortical accumulation was evaluated as 1 (good). Too smoothed or too noisy accumulation of the cortex was evaluated as 0 (poor). For the caudate and the thalamus, clear contour and homogeneous accumulation was 1, and too smooth contour or too noisy accumulation was 0. Clear separation of the lingual gyri of the right and left hemispheres was 1, and too smooth or unclear separation due to image noise was 0. Scores were summed for each image and compared with visually determined optimal cutoff frequencies.

Relationship between total counts and optimal cutoff frequencies

The number of counts in every projection was summed in each projection set to represent total counts of the study. Optimal cutoff frequencies determined by the MSE and visual inspection for each projection set were compared with the total counts.

RESULTS

High quality standard image

High quality images created from high-count projections had a high image quality with a wide range of cutoff frequencies of the Butterworth filter. Images reconstructed using the cutoff frequencies of 0.13, 0.14, and 0.15 cycles/pixel were determined as the best images to show suitable smoothing of the cortical accumulation and clear visualization of the caudate and the thalamus (Fig. 3). These three images were used as the high quality standard images in the following analysis.

Optimization by MSE

Each projection set had a unique minimum of the MSE calculated from each high quality standard image. A cutoff frequency giving the MSE minimum was determined as the optimal cutoff frequency. In this study, the optimal cutoff frequencies determined by mean of the three different high quality standard images showed the same values in each projection set: 0.08 cycles/pixel for 20-second, 0.09 for 40-second, 0.10 for 60-second, 0.11 for 80-second, and 0.11 for 100-second acquisition (Fig. 4). With increasing acquisition time, the optimal cutoff frequency increased.

Optimization by visual inspection

Optimal cutoff frequencies determined by visual inspections were 0.07 cycles/pixel for 20-second, 0.09 for 40-second, 0.10 for 60-second, 0.11 for 80-second, and 0.12 for 100-second acquisition (Fig. 5). With increasing acquisition time, the visually-determined optimal cutoff frequency increased.

The range of cutoff frequencies which yielded reconstructed images with a score of 4 became wider with increasing acquisition time (Fig. 5). In 20-second acquisition, score-4 images could not be generated using any cutoff frequency. Visually determined optimal cutoff frequencies were located approximately at the center of the range of the cutoff frequencies which yielded score-4 images.

Relationship between total counts and optimal cutoff frequencies

As total counts increased, the optimal cutoff frequencies determined by the MSE and visual inspection linearly increased within a given range of total counts. The optimal cutoff frequencies determined by the two methods showed an approximately equivalent relationship with total counts. (Fig. 6).

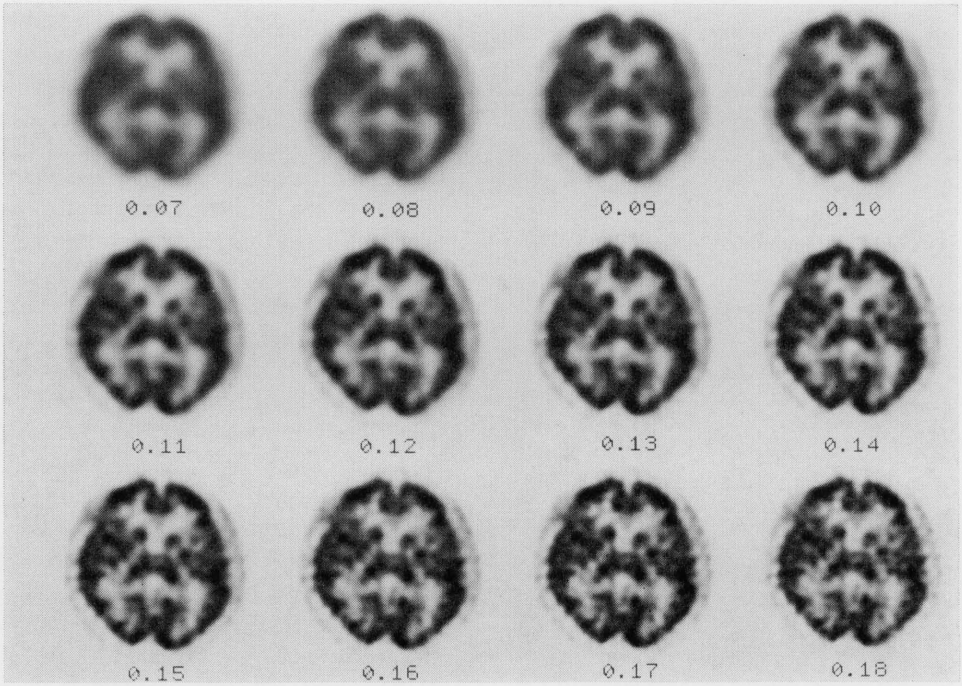

Fig. 3 High quality standard images. Images were created from a 300-second projection set with cutoff frequencies of a Butterworth filter from 0.07 to 0.18 cycles/pixel. Images obtained by cutoff frequencies of 0.13, 0.14, and 0.15 cycles/pixel were determined as a high quality standard image according to visual inspections of two experienced observers.

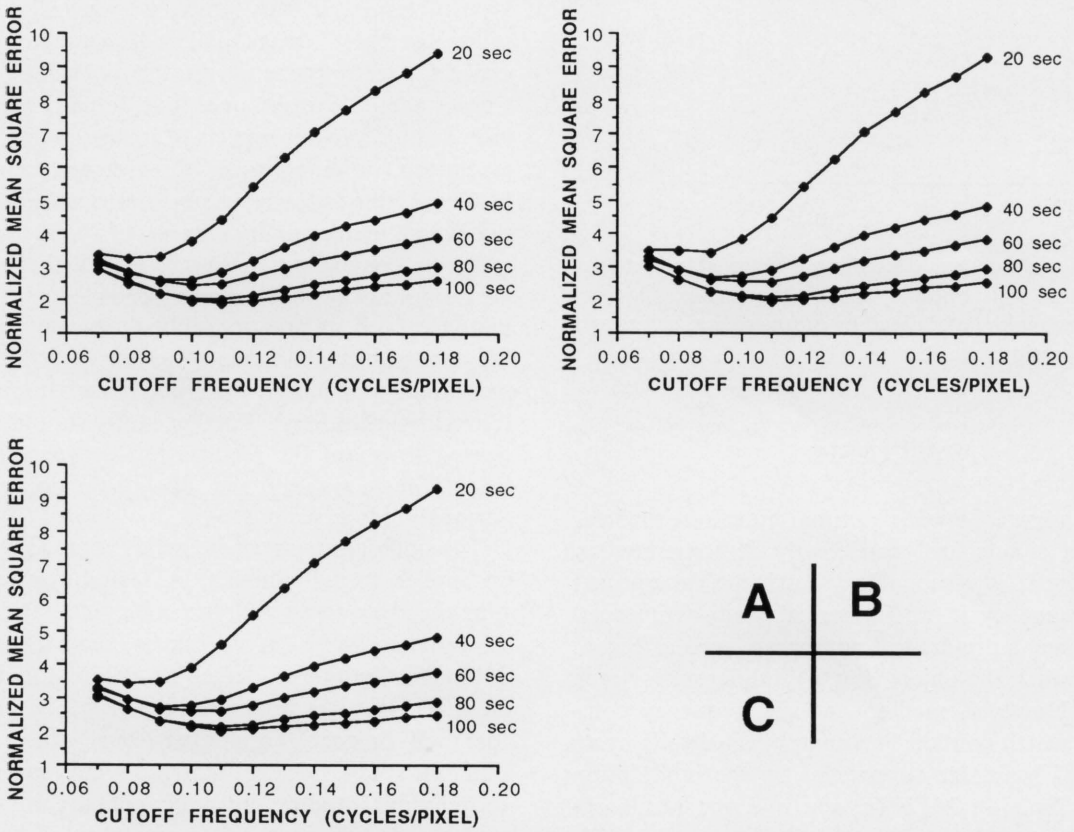

Fig. 4 Relationship between different acquisition time, cutoff frequencies, and mean square errors calculated from high quality standard images. High quality standard images obtained by cutoff frequencies of 0.13, 0.14, and 0.15 cycles/pixel were used in A, B, and C, respectively.

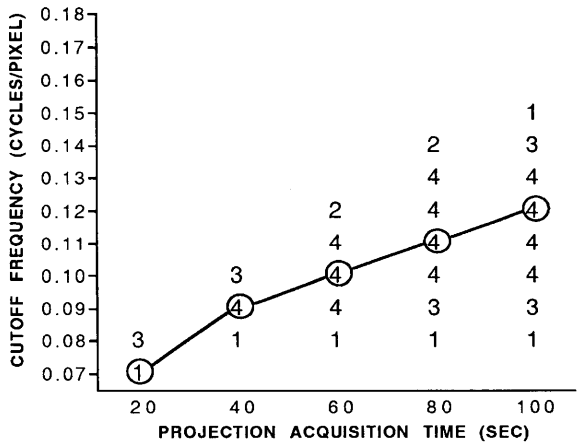

Fig. 5 Relationship between different acquisition time, cutoff frequencies, and visual inspections. Numbers are summation of scores obtained from visual inspections of four check points. Score 0 is omitted. Circled numbers indicate "best" images determined by visual inspections of two experienced observers.

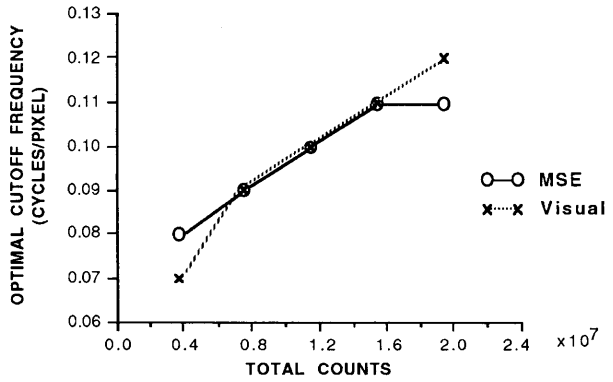

Fig. 6 A nomogram describing relationship between total counts and optimal cutoff frequencies. Optimal cutoff frequencies determined by means square errors and visual inspections are shown.

DISCUSSION

As dependence between optimal cutoff frequencies and total counts has been clearly demonstrated in this study, it is reasonable to estimate an optimal cutoff frequency in an individual study from total counts using a pre-defined nomogram such as Fig. 6. In equation 1, the object F (u, v) is different for each subject. However, medium-to-high frequency components which contain fine anatomical details of an individual brain are suppressed by the modulation transfer function MTF (u, v),[7] and the result obtained from a single subject will give a reasonable approximation for different subjects. King et al. have reported count-dependent Metz filter optimization using Alderson Organ Scanning Phantom data.[6] They have found that the result obtained from the phantom data was a good approximation for a number of applications even if target organ shapes were different from the phantom shape. The estimated cutoff frequency can be further adjusted, if necessary, using an interactive visual inspection system.[8]

Although the filter has been optimized for visual interpretation in this study, it is important to clarify the purpose of the optimization. If the purpose of the optimization is quantitative data analysis, a filter should be optimized in terms of quantitative accuracy. Image contrast[9] and image resolution[10] can be used as optimization indices for restoration filters. Lesion detectability is another index for filter optimization. Receiver operating characteristic (ROC) analysis for specific lesions has been used to optimize various filters.[6,11] However, lesion size, shape, and activity should be taken into account when optimizing filters because different lesions have different spatial-frequency components. For example, a filter optimized to detect a 20 mm defect in the temporal lobe is not necessarily optimal to detect a slight reduction of cerebral blood flow in the territory of the middle cerebral artery. When using linear filtering and reconstruction techniques, it is difficult to optimize lesion detectability for every type of lesion. In this study, we basically used an index, the "best" image quality determined by expert observers to optimize the Butterworth filter. Definition of the best image quality is actually vague and may include various aspects of image quality such as resolution, noise, contrast, observer preference, etc.. However, this index is reasonable because it reflects the overall image quality in terms of visual inspection which is convincing to observers. Furthermore, as we do not always have *a priori* knowledge of lesions in images, it is, in practice, difficult to optimize filters for each subject in terms of lesion detectability (as mentioned previously, different lesions require different optimizations). Further study should be conducted to reveal the relationship between the optimized image quality and diagnostic accuracy for various kinds of lesions.

The nomogram obtained in this study (Fig. 6) can be applied to individual SPECT studies when scanning the same organ with the same modulation transfer function MTF (u, v) (that is, the same camera, collimator, radionuclide, object-collimator distance, etc.). Practically, nomograms should be prepared for each protocol (brain perfusion study, cardiac thallium study, liver colloid study, etc.) and applied to individual studies. If total counts are not variable under a certain protocol, a single cutoff frequency may be applicable to every study. To obtain the nomogram in this study, ^{99m}Tc HMPAO and a normal volunteer were used because of its stable

distribution in the brain after the initial uptake[12] and a realistic F (u, v) of the brain, respectively. Instead, an anatomically accurate phantom can be used to replicate the method presented in this study. For example, a nomogram for brain perfusion studies can be obtained using a three dimensional brain phantom[13] filled with ^{99m}Tc or ^{123}I and projection sets with different total counts. The MSE approach with a high quality image created from high-count projections and/or visual inspection approach for individual filtered images can be applied to optimize filters. Both approaches yielded equally effective results in this study. Also, this type of nomogram can be implemented for commercial systems or provided with systems for possible imaging protocols as a guide to filter determination. Determination of a filter function according to a certain rule is important not only for optimizing individual images but also for comparing multiple images. Along with reconstruction methods, filtering in SPECT imaging should be further validated and optimized to yield consistent image quality for visual diagnostic purposes.

ACKNOWLEDGMENTS

The authors thank Kouichi Ogawa, Ph.D., Keio University Division of Nuclear Medicine, for helpful discussions.

REFERENCES

1. Kimura K, Hashikawa K, Etani H, et al: A new apparatus for brain imaging: four-head rotating gamma camera single-photon emission computed tomograph. *J Nucl Med* 31: 603–609, 1990
2. Holman BL, Carvalho PA, Zimmerman RE, et al: Brain perfusion SPECT using an annular single crystal camera: initial clinical experience. *J Nucl Med* 31: 1456–1461, 1990
3. Matsuda H, Oskoie SD, Kinuya K, et al: Tc-99m HMPAO brain perfusion tomography atlas using a high resolution SPECT system. *Clin Nucl Med* 15: 428–431, 1990
4. Mountz JM, Rogers WL, Wilson MW, et al: Clinical SPRINT imaging, preliminary results compared to conventional SPECT brain scanning using Tc-99m HMPAO. *Clin Nucl Med* 16: 562–567, 1991
5. Budinger TF, Gullberg GT, Huesman RH: Image reconstruction from projections. Herman GT, (ed.), New York, Springer-Verlag, p197, 1979
6. King MA, Doherty PW, Schwinger RB, et al: Fast count-dependent digital filtering of nuclear medicine images: concise communication. *J Nucl Med* 24: 1039–1045, 1983
7. Madsen MT, Park CH: Enhancement of SPECT images by Fourier filtering the projection image set. *J Nucl Med* 26: 395–402, 1985
8. King, MA, Glick SJ, Penney BC, et al: Interactive visual optimization of SPECT prereconstruction filtering. *J Nucl Med* 28: 1192–1198, 1987
9. King MA, Schwinger RB, Doherty PW, et al: Two-dimensional filtering of SPECT images using the Metz and Wiener filters. *J Nucl Med* 25: 1234–1240, 1984
10. King MA, Schwinger RB, Penney BC, et al: Digital restoration of Indium-111 and Iodine-123 SPECT images with optimized Metz filters. *J Nucl Med* 27: 1327–1336, 1986
11. Gilland DR, Tsui BMW, McCartney WH, et al: Determination of the optimum filter function for SPECT imaging. *J Nucl Med* 29: 643–650, 1988
12. Neirinckx RD, Canning LR, Piper IM, et al: Technetium-99m d, l-HM-PAO: a new radiopharmaceutical for SPECT imaging of regional cerebral blood perfusion. *J Nucl Med* 28: 191–202, 1987
13. Hoffman EJ, Cutler PD, Digby WM, et al: 3-D phantom to simulate cerebral blood flow and metabolic images for PET. *IEEE Trans Nuc Sci* NS-37 (20): 616–620, 1990